Available online at www.sciencedirect.com
SCIENCE DIRECT
Polymer 47 (2006) 639–651
polymer
www.elsevier.com/locate/polymer

Comparison of the toughening behavior of nylon 6 versus an amorphous polyamide using various maleated elastomers

J.J. Huang, H. Keskkula, D.R. Paul *

Department of Chemical Engineering, Texas Materials Institute, The University of Texas at Austin, Austin, TX 78712-1062, USA

Received 4 October 2005; received in revised form 30 November 2005; accepted 30 November 2005

Abstract

The toughening effect of two types of elastomers based on ethylene/α-olefin copolymers, viz, an ethylene/propylene copolymer (EPR) with its maleated version, EPR-*g*-MA, and an ethylene/1-octene copolymer (EOR) with its maleated versions, EOR-*g*-MA-*X*% ($X=0.35$, 1.6, 2.5), for two classes of polyamides: semi-crystalline nylon 6 versus an amorphous polyamide (Zytel 330 from DuPont), designated as a-PA, was explored. The results are compared with those reported earlier based on a styrenic triblock copolymer having a hydrogenated midblock, SEBS, and its maleated version, SEBS-*g*-MA, elastomer system. Izod impact strength was examined as a function of rubber content, rubber particle size and temperature. All three factors influence the impact behavior considerably for the two polyamide matrices. The a-PA is found to require a somewhat lower content of rubber for toughening than nylon 6. Very similar optimum ranges of rubber particle sizes were observed for ternary blends of EOR-*g*-MA/EOR with each of the two polyamides while blends based on mixtures of EPR-*g*-MA/EPR and SEBS-*g*-MA/SEBS (where the total rubber content is 20% by weight) show only an upper limit for a-PA but an optimum range of particle sizes for nylon 6 for effective toughening. Higher EPR-*g*-MA contents lead to lower ductile–brittle transition temperatures (T_{db}) as expected; however, a-PA binary blends with EPR-*g*-MA have a much lower T_{db} than do nylon 6 blends when the content of the maleated elastomer is not high. A minimum in plots of ductile–brittle transition temperature versus particle size appears for ternary blends of each of the matrices with EOR-*g*-MA/EOR; blends based on SEBS-*g*-MA/SEBS, in most cases, show higher ductile–brittle transition temperatures, regardless of the matrix. However, blends with EPR-*g*-MA/EPR show comparable T_{db} with those based on EOR-*g*-MA/EOR for the amorphous polyamide but show the lowest ductile–brittle transition temperatures for nylon 6 within the range of particle sizes examined. For the blends with a bimodal size distribution, the global weight average rubber particle size is inappropriate for correlating the Izod impact strength and ductile–brittle transition temperature. In general, trends for this amorphous polyamide are rather similar to those of semi-crystalline nylon 6.
© 2005 Elsevier Ltd. All rights reserved.

Keywords: Amorphous polyamide; Impact strength; Toughening

1. Introduction

Numerous studies have been reported on the rubber toughening of semi-crystalline polyamides like nylon 6 and nylon 66 using maleated elastomers [1–21]. By contrast, there are relatively few reports on rubber toughening of amorphous polyamides [22–24]. We recently initiated such studies primarily motivated by our interest in obtaining a better understanding of the toughening mechanisms of semi-crystalline polyamides by comparing the toughening responses of an amorphous matrix using the same elastomers [24]. In an earlier paper [25], we described the elastomer particle morphology for ternary blends of maleated and non-maleated ethylene-based elastomers with nylon 6 and an amorphous polyamide, Zytel 330 from DuPont. The elastomers used include an ethylene/propylene copolymer (EPR) with its maleic anhydride (MA) grafted version EPR-*g*-MA, and an ethylene/1-octene copolymer (EOR) with its maleated versions, EOR-*g*-MA-*X*% where *X* is 0.35, 1.6 and 2.5. Specifically, we have demonstrated when using mixtures of elastomers with different levels of maleation for achieving fine control of rubber particle sizes that elastomer phase miscibility becomes a significant factor in the morphology formed in addition to factors like the ratio of the two elastomers, the matrix type, the order of mixing and the mixing intensity (the extruder type), etc. In some cases, bimodal distributions of particle sizes were observed [25]. Obviously, the morphology of the resulting polyamide blend is a major factor in determining the final mechanical properties including Izod impact strength. The purpose of this paper is to report in some detail the toughening response of these two

* Corresponding author. Tel.: +1 512 471 5392; fax: +1 512 471 0542.
E-mail address: drp@che.utexas.edu (D.R. Paul).

0032-3861/$ - see front matter © 2005 Elsevier Ltd. All rights reserved.
doi:10.1016/j.polymer.2005.11.088

classes of polyamide matrices using these two types of elastomers. The effect of rubber content and particle size on Izod impact strength and the ductile–brittle transition temperature will be presented. A final paper [26] will explore the fracture behavior of selected blends in more detailed ways.

2. Experimental section

Table 1 shows the physical and mechanical properties of the materials employed in this study. The procedures for melt blending and morphology determination have been fully described elsewhere [25].

Standard tensile and Izod impact specimens, 0.318 cm thick, were formed using an Arburg Allrounder injection molding machine from blends containing 20 wt% rubber phase and 80 wt% polyamide matrix. The samples were tested 'dry as molded' using standard tensile (ASTM D638) and Izod (ASTM D256) procedures. Tensile testing was performed using an Instron model 1137. Modulus and yield stress were determined at a crosshead rate of 0.51 cm/min while elongation at break data were collected at 5.1 cm/min. Izod impact testing was done using a TMI Impact Tester (model 43-02) equipped with a thermal chamber so that the samples could be tested at a variety of temperatures. The testing procedures are given elsewhere [16]. The tested samples failed in three modes: a hinged break when tested above the ductile–brittle transition temperature, a complete break into two pieces when tested below the ductile–brittle transition temperature and a mixed mode in the ductile–brittle transition region where specimens of the same composition showed either a hinged or a complete break.

The dynamic mechanical properties of injection molded (3.18 mm thick) specimens of neat a-PA and nylon 6 materials and the neat elastomers employed in this work were determined by a Rheometric Scientific Dynamic Mechanical Thermal Analyser (DMTA) Mk III at a frequency of 1 Hz, a strain level setting of 4 which corresponds to about 0.07% strain, and under a single cantilever mode. All samples were cooled with liquid nitrogen to −100 °C and heated at a rate of 2 °C/min. The DMTA was calibrated prior to all testing.

3. Room temperature mechanical properties

3.1. Tensile properties

Table 2 summarizes the mechanical properties of binary blends of each of the two polyamides with EPR-*g*-MA. As can be seen, modulus and yield stress are steadily reduced by the addition of EPR-*g*-MA. The elongation at break is rather erratic owing to a variety of issues that have been discussed in previous papers on similar blends [7,24]. Table 3 shows the mechanical properties of ternary blends of a-PA containing a total of 20 wt% rubber comprised of mixtures of EPR-*g*-MA

Table 1
Materials used

Designation used here	Materials (commercial designation)	Compositions	T_g (°C)[a]	Elastic modulus (MPa)[b]	MFR (g/10 min)[c]	Brabender torque (N m)[d]	Supplier
a-PA	Zytel 330[e]		127	1597		10.7	DuPont
Nylon 6[f]	B73WP[g]		55	1804		6.37[h]	Honeywell
EOR	Exact 8201	28 wt% octene	−34	24.1	~22	9.5	ExxonMobil
EOR-*g*-MA-0.35%	Exxelor VA 1840	28 wt% octene 0.35 wt% MA	−31	25.3	~25	9.2	ExxonMobil
EOR-*g*-MA-1.6%	Exxelor MDEX 101-2	28 wt% octene 1.6 wt% MA	−28	29.3	19	6.9	ExxonMobil
EOR-*g*-MA-2.5%	Exxelor MDEX 101-3	28 wt% octene 2.5 wt% MA	−28	29.7	20	6.3	ExxonMobil
EPR	Vistalon 457	53 wt% propylene	~−47	N/A		14.2[h]	ExxonMobil
EPR-*g*-MA	Exxelor 1803	53 wt% propylene 1.14 wt% MA	−47	3.2		9.76[h]	ExxonMobil
SEBS	Kraton G 1652	29 wt% styrene	~−36	40		8.58	Kraton Polymers
SEBS-*g*-MA	Kraton G 1901X	29 wt% styrene 1.84 wt% MA	−36	66		6.37	Kraton polymers

[a] Data measured from the tan δ peak of DMTA.
[b] Data measured by the DMTA at 1 Hz and 25 °C.
[c] Data at 230 °C and 10 kg and provided by the supplier.
[d] Measured after 10 min at 240 °C and 60 rpm.
[e] 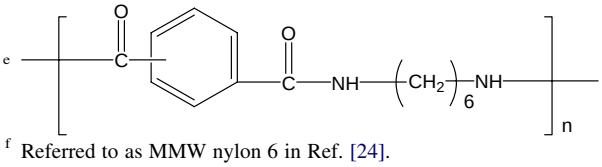

[f] Referred to as MMW nylon 6 in Ref. [24].
[g] Formerly Capron 8207F.
[h] Data from Ref. [15].

Table 2
Summary of rubber particle size and mechanical properties for binary blends of polyamides with EPR-*g*-MA

Matrix	Rubber (wt%)	Extruder type	$\bar{d}_w$ (μm)	$\bar{d}_w/\bar{d}_n$	$\bar{d}_v/\bar{d}_n$	Izod impact (J/m)	T_{db} (°C)	Modulus (GPa)	Yield stress (MPa)	Elongation at break (%)
a-PA	0	Twin				23	N/A	2.7	92.1	116
	5	Twin	0.14	1.22	1.73	249	30	2.4	79.6	62
	7.5	Twin	0.17	1.14	1.51	958	0	2.4	74.5	90
	10	Twin	0.18	1.15	1.54	833	−20	2.2	70.7	48
	12.5	Twin	0.16	1.11	1.39	866	−30	2.2	66.9	102
	15	Twin	0.19	1.17	1.68	758	−30	1.8	62.5	44
	20	Twin	0.20	1.18	1.70	726	−35	1.8	56.1	33
Nylon 6	0[a]	Single				43	N/A	2.8	70.2	93
	5	Single	0.288	1.85	5.2	95	65	2.4	63.1	9
	10	Single	0.157	1.32	2.06	183	35	2.4	58.7	22
	15	Single	0.175	1.47	3.27	238	−20	2.1	52.6	24
	20	Single	0.20	1.42	2.72	619	−35	1.9	46.7	49

[a] Data from Ref. [16].

and EPR in different proportions. Modulus and yield stress change by 10 and 7.5%, respectively. Elongation at break varies more than modulus and yield stress.

Tables 4 and 5 summarize the mechanical properties for blends of nylon 6 and a-PA with various mixtures of EOR-*g*-MA and EOR. Modulus and yield stress change by up to 16%. The standard deviation for the measurement of modulus is less than 5% and less than 1% for yield stress. Elongation at break changes significantly from one blend to another and also, the standard deviation is much greater, sometimes, of the order of 50% or even higher.

3.2. Izod impact strength

Fig. 1 shows the Izod impact strength as a function of EPR-*g*-MA content for binary blends where the matrix polyamide is a-PA and nylon 6. Interestingly, the toughness of nylon 6 as measured by the Izod value increases gradually with EPR-*g*-MA content up to about 15 wt% and then appears to level off. On the other hand, there is a dramatic rise in Izod value between 5 and 7.5 wt% EPR-*g*-MA for the a-PA system followed by a gradual decline at higher rubber contents which approaches the plateau value for nylon 6. To some extent the decrease in Izod value in the latter region parallels the large change in yield strength observed, see Table 2. However, one should be cautious about drawing broad conclusions regarding the toughenability of the two matrices by comparing toughness levels between a-PA and nylon 6 at any given EPR-*g*-MA content since these plots do not represent optimized rubber particle sizes.

Fig. 2 shows the effect of rubber particle size on the Izod impact strength for ternary blends based on mixtures of EOR-*g*-MA and EOR for each of the two types of polyamides where the total rubber content is fixed at 20 wt%. In cases where the rubber particle size distribution shows bimodality, the Izod value is plotted at the global weight average size for the entire particle size distribution. For specimens that showed differences in toughness at the gate and far ends of the Izod bar, both Izod values are plotted. For a-PA, an upper limit on rubber particle size of about 0.7 μm is seen beyond which the blend is brittle. As the particle size is within a range of 0.4–0.75 μm, the far end specimens appear much tougher than the gate end samples. Similar cases have been reported for ternary blends of a-PA with maleated and non-maleated SEBS [24] and were attributed to the highly elongated rubber phase morphology in the gate end part of the specimen. For the blends exhibiting bimodality in morphology, a much lower impact strength is generally observed when compared, using the global average particle size, with cases where the particle size distribution is unimodal. Interestingly, two blends with bimodal particle size distributions do appear to be super-tough. For nylon 6, the optimum range of rubber particle sizes for super-toughness is 0.15–0.8 μm. A similar optimum range of rubber particle sizes for nylon 6 has been observed in ternary blends with maleated and non-maleated SEBS [7,16].

For nylon 6, unlike the case of a-PA, all the blends with a bimodal distribution of particle sizes appear to be super-tough.

Table 3
Summary of mechanical properties for ternary blends of 80 wt% a-PA with 20 wt% EPR-*g*-MA/EPR

EPR-*g*-MA wt% in rubber phase	%MA in the rubber phase	$\bar{d}_w$ (μm)	$\bar{d}_w/\bar{d}_n$	$\bar{d}_v/\bar{d}_n$	Izod impact (J/m)	T_{db} (°C)	Modulus (GPa)	Yield stress (MPa)	Elongation at break (%)
20	0.23	0.44	1.51	2.58	344	0	2.0	60.6	21
60	0.68	0.28	1.39	2.81	642	−25	1.8	57.7	28
100	1.14	0.20	1.18	1.70	726	−35	1.8	56.1	33

Table 4
Summary of rubber particle sizes and mechanical properties for blends of a-PA based on EOR-*g*-MA/EOR

MA%	Rubber phase (20%)	Order of mixing	$\bar{d}_w$ (μm)	$\bar{d}_w/\bar{d}_n$	$\bar{d}_v/\bar{d}_n$	ID_w[a]	Izod impact (J/m)	T_{bd} (°C)	Modulus (GPa)	Yield stress (MPa)	Elongation at break (%)
0	EOR	Simultaneous	2.41	1.26	1.78	0.67	70	N/A	1.7	N/A[b]	6
0.035	EOR-*g*-MA-0.35%/EOR = 10:90	Simultaneous	1.10	1.56	2.51	0.31	108	N/A	2.0	57.3	10
0.0875	EOR-*g*-MA-0.35%/EOR = 25:75	Simultaneous	0.75	1.59	2.94	0.21	732 far 254 gate	25	2.0	57.2	44
		Premixed	0.78	1.90	2.39	0.22	246	35	1.8	59.7	23
0.14	EOR-*g*-MA-0.35%/EOR = 40:60	Simultaneous	0.50	1.63	3.44	0.14	963 far 426 gate	10	1.7	53.9	71
0.28	EOR-*g*-MA-0.35%/EOR = 80:20	Simultaneous	0.31	1.32	3.45	0.09	1060	−5	1.6	50.1	163
		Master batch	0.28	1.39	3.82	0.08	1076	−20	1.7	53.1	173
0.35	EOR-*g*-MA-0.35%	Simultaneous	0.35	1.39	2.83	0.10	1108	−25	1.7	53.5	146
0.39	EOR-*g*-MA-1.6%/EOR = 24:76	Simultaneous	0.26	1.94	9.67	0.07	646	0	1.8	55.8	11
		Premixed	0.20	1.66	5.16	0.06	827	0	1.7	55.1	29
	EOR-*g*-MA-2.5%/EOR = 16:84	Simultaneous	0.27	2.79	11.7	0.08	221	30	1.7	51.2	8
0.44	EOR-*g*-MA-1.6%/EOR = 28:72	Simultaneous	0.25	1.94	9.68	0.07	637	−5	1.7	54.9	11
	EOR-*g*-MA-2.5%/EOR = 18:82	Simultaneous	0.25	2.67	13.7	0.07	352	25	1.8	52.3	8
		Premixed	0.24	2.63	17.2	0.07	477	15	1.8	54.4	10
0.48	EOR-*g*-MA-1.6%/EOR = 30:70	Simultaneous	0.19	1.32	2.82	0.05	812	45	1.8	54.3	43
	EOR-*g*-MA-2.5%/EOR = 19:81	Simultaneous	0.20	2.20	10.05	0.06	430	15	1.7	52.5	9
0.5375	EOR-*g*-MA-1.6%/EOR-*g*-MA-0.35% = 15:85	Simultaneous	0.26	1.39	3.14	0.07	1104	−30	1.8	55.4	159
0.6725	EOR-*g*-MA-2.5%/EOR-*g*-MA-0.35% = 15:85	Simultaneous	0.23	1.45	4.54	0.06	1080	−30	1.7	52.9	170
0.85	EOR-*g*-MA-1.6%/EOR-*g*-MA-0.35% = 40:60	Simultaneous	0.13	1.13	1.44	0.04	1000	−30	1.7	56.5	88
0.96	EOR-*g*-MA-1.6%/EOR = 60:40	Simultaneous	0.15	1.16	1.55	0.04	998	−20	1.7	55.4	147
1.0	EOR-*g*-MA-2.5%/EOR = 40:60	Simultaneous	0.13	1.30	3.04	0.04	842	−10	1.8	55.6	61
1.21	EOR-*g*-MA-2.5%/EOR-*g*-MA-0.35% = 40:60	Simultaneous	0.10	1.23	1.53	0.03	1015	−30	1.7	56.2	64
1.225	EOR-*g*-MA-1.6%/EOR-*g*-MA-0.35% = 70:30	Simultaneous	0.14	1.10	1.33	0.04	993	−30	1.6	55.9	75
1.5	EOR-*g*-MA-2.5%/EOR = 60:40	Simultaneous	0.11	1.21	1.57	0.03	959	−30	1.7	54.7	64
		Master batch	0.11	1.20	1.74	0.03	952	−30	1.7	54.7	72
1.6	EOR-*g*-MA-1.6%	Simultaneous	0.14	1.26	1.96	0.04	969	−30	1.7	53.2	158
1.735	EOR-*g*-MA-2.5%/EOR-*g*-MA-1.6% = 15:85	Simultaneous	0.16	1.21	1.86	0.05	931	−30	1.7	53.8	147
1.855	EOR-*g*-MA-2.5%/EOR-*g*-MA-0.35% = 70:30	Simultaneous	0.11	1.16	1.68	0.03	972	−30	1.9	54.8	32
1.96	EOR-*g*-MA-2.5%/EOR-*g*-MA-1.6% = 40:60	Simultaneous	0.12	1.12	1.42	0.03	965	−30	1.7	56.6	38
2.23	EOR-*g*-MA-2.5%/EOR-*g*-MA-1.6% = 70:30	Simultaneous	0.12	1.13	1.45	0.04	939	−30	1.7	57.1	52
2.5	EOR-*g*-MA-2.5%	Simultaneous	0.13	1.20	1.64	0.04	888	−25	1.7	53.7	131

[a] Weight average interparticle distance based on Wu's model [3].
[b] Break before yielding.

Table 5
Summary of rubber particle sizes and mechanical properties for blends of nylon 6 based on EOR-*g*-MA/EOR

MA%	Rubber phase (20%)	Extruder	Order of mixing	$\bar{d}_w$ (μm)	$\bar{d}_w/\bar{d}_n$	$\bar{d}_v/\bar{d}_n$	ID_w[a]	Izod impact (J/m)	T_{db} (°C)	Modulus (GPa)	Yield stress (MPa)	Elongation at break (%)
0	EOR	Twin	Simultaneous	2.70	1.37	1.72	0.78	74	55	2.0	51.8	23
0.021	EOR-*g*-MA-0.35%/EOR = 6:94	Twin	Simultaneous	1.19	1.90	3.55	0.35	120	45	2.2	52.4	30
0.042	EOR-*g*-MA-0.35%/EOR = 12:88	Twin	Simultaneous	0.85	1.64	3.07	0.25	563	20	2.0	49.3	50
0.05845	EOR-*g*-MA-0.35%/EOR = 17:83	Twin	Simultaneous	0.38	1.65	3.52	0.11	815	10	1.8	44.9	113
		Twin	Premixed	0.36	1.56	3.54	0.11	733	0	2.1	48.8	63
		Twin	Master batch	0.42	1.39	2.11	0.12	725	0	2.0	48.8	88
		Single	Simultaneous	0.54	1.83	3.64	0.16	652	20	2.0	48.8	147
		Single	Master batch	0.58	1.97	4.63	0.17	198	35	2.0	50.2	116
0.14	EOR-*g*-MA-0.35%/EOR = 40:60	Twin	Simultaneous	0.20	1.34	2.98	0.058	661	−10	1.9	48.2	96
0.21	EOR-*g*-MA-0.35%/EOR = 60:40	Single	Master batch	0.37	1.53	3.42	0.11	857	−20	1.8	47.2	124
		Twin	Simultaneous	0.15	1.21	2.02	0.042	460	−15	1.7	45.7	141
			Master batch	0.16	1.18	1.65	0.047	493	−20	1.8	48.0	141
0.35	EOR-*g*-MA-0.35%	Twin	Simultaneous	0.10	1.10	1.44	0.028	323	−10	1.9	51.5	101
0.39	EOR-*g*-MA-1.6%/EOR = 24:76	Twin	Simultaneous	0.19	1.85	6.08	0.055	677	−10	1.9	50.3	77
			Premixed	0.18	1.69	4.89	0.054	490	−10	2.0	48.6	90
			Master batch	0.15	1.83	6.04	0.043	566	−5	1.9	48.1	136
	EOR-*g*-MA-2.5%/EOR = 16:84	Twin	Simultaneous	0.21	2.34	8.82	0.062	694	10	1.9	50.9	44
0.44	EOR-*g*-MA-1.6%/EOR = 28:72	Twin	Simultaneous	0.15	1.67	7.26	0.043	645	−5	2.0	51.3	159
	EOR-*g*-MA-2.5%/EOR = 18:82	Twin	Simultaneous	0.19	2.43	13.25	0.057	642	15	2.1	52.8	51
		Twin	Premixed	0.17	1.96	7.95	0.048	591	0	2.0	49.1	144
		Twin	Master batch	0.18	2.14	7.10	0.052	646	10	2.0	48.1	86
		Single	Master batch	0.42	2.89	9.30	0.12	441	25	2.0	48.6	55
0.48	EOR-*g*-MA-1.6%/EOR = 30:70	Twin	Simultaneous	0.14	1.49	5.80	0.040	577	−10	2.0	53.8	128
	EOR-*g*-MA-2.5%/EOR = 19:81	Twin	Simultaneous	0.16	1.89	7.0	0.046	708	15	2.0	52.1	206
0.5375	EOR-*g*-MA-1.6%/EOR-*g*-MA-0.35% = 15:85	Twin	Simultaneous	0.083	1.17	1.82	0.024	247	0	1.8	46.6	136
0.6725	EOR-*g*-MA-2.5%/EOR-*g*-MA-0.35% = 15:85	Twin	Simultaneous	0.078	1.16	1.55	0.023	263	0	2.0	50.5	117
0.85	EOR-*g*-MA-1.6%/EOR-*g*-MA-0.35% = 40:60	Twin	Simultaneous	0.064	1.14	1.57	0.019	253	−20	1.9	48.7	144
1.21	EOR-*g*-MA-2.5%/EOR-*g*-MA-0.35% = 40:60	Twin	Simultaneous	0.068	1.11	1.38	0.020	259	−15	1.8	47.6	192
1.225	EOR-*g*-MA-1.6%/EOR-*g*-MA-0.35% = 70:30	Twin	Simultaneous	0.057	1.14	1.48	0.017	225	−10	2.0	51.5	116
1.5	EOR-*g*-MA-2.5%/EOR = 60:40	Single	Master batch	0.095	1.53	3.65	0.028	631	−20	1.8	47.3	75
		Twin	Simultaneous	0.062	1.22	2.04	0.018	353	−10	1.8	47.0	140
			Master batch	0.057	1.16	1.78	0.017	309	−10	1.8	46.4	191
1.6	EOR-*g*-MA-1.6%	Twin	Simultaneous	0.051	1.10	1.40	0.015	247	0	2.0	51.9	61
1.735	EOR-*g*-MA-2.5%/EOR-*g*-MA-1.6% = 15:85	Twin	Simultaneous	0.049	1.14	1.63	0.014	221	5	1.7	45.1	211
1.855	EOR-*g*-MA-2.5%/EOR-*g*-MA-0.35% = 70:30	Twin	Simultaneous	0.047	1.18	1.68	0.014	255	−10	1.8	46.6	136
1.96	EOR-*g*-MA-2.5%/EOR-*g*-MA-1.6% = 40:60	Twin	Simultaneous	0.049	1.14	1.56	0.014	214	0	1.8	48.1	200
2.23	EOR-*g*-MA-2.5%/EOR-*g*-MA-1.6% = 70:30	Twin	Simultaneous	0.045	1.22	1.78	0.013	250	0	1.8	47.2	179
2.5	EOR-*g*-MA-2.5%	Twin	Simultaneous	0.043	1.16	1.73	0.013	234	0	1.9	48.2	180

[a] Weight average interparticle distance based on Wu's model [3].

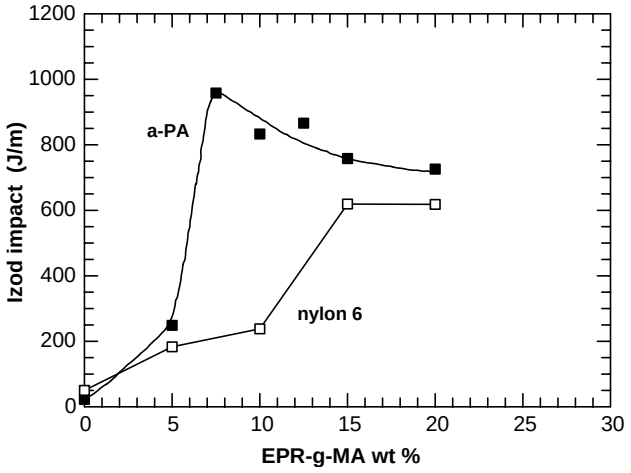

Fig. 1. Comparison of the Izod impact strength of binary blends of EPR-*g*-MA with a-PA and with nylon 6 as a function of total rubber content.

The optimum rubber particle size for toughening is roughly the same for the two polyamide matrices. At this optimum size, the Izod values for a-PA are about 20–30% higher than those for nylon 6. As shown in Figs. 1 and 2, the amorphous polyamide is similar qualitatively to nylon 6 but is different quantitatively in some situations where the amorphous polyamide seems to be more easily toughened than does nylon 6. The larger size of the deformation zone observed in the a-PA blend than in the nylon 6 blend exhibiting the highest impact strength (1108 J/m for a-PA and 815 J/m for nylon 6) mainly accounts for the differences between the two polyamides. Such differences may stem from numerous sources including the fact that one is entirely amorphous while the other is semi-crystalline with a crystallinity of about 50%. The toughening response is a complex process where yield strength, viscoelastic behavior, and other matrix effects in addition to blend morphology all play some role.

It is instructive to re-examine the toughness of blends with bimodal particle sizes in another way. For the blends exhibiting bimodality in morphology, a weight average particle diameter was estimated for each of the populations so that there are two average rubber particle diameters for each of the blends. The single value of impact strength of a blend with a bimodal size distribution is entered in Fig. 3 both at the weight average size

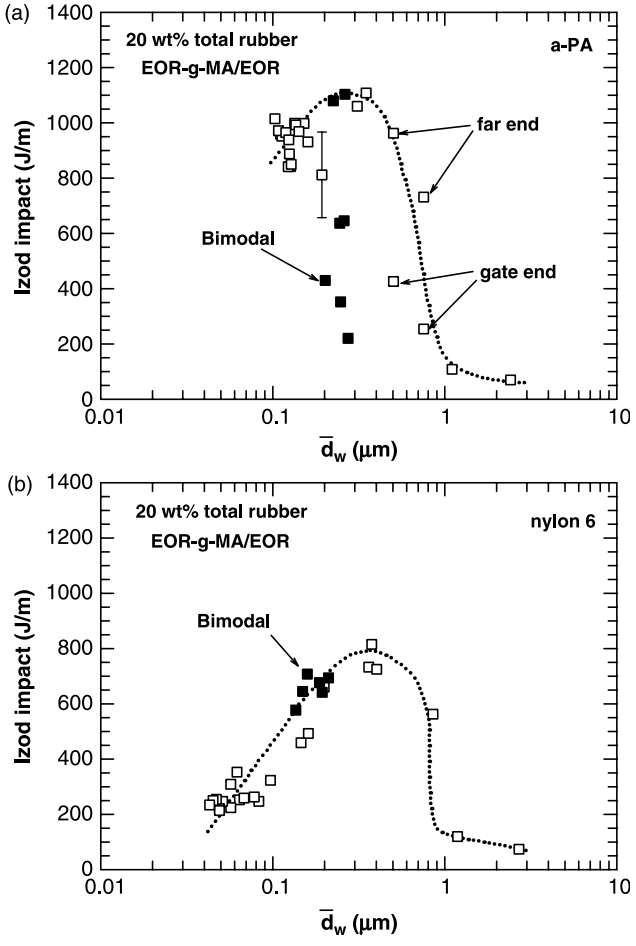

Fig. 2. Effect of the global average rubber particle size on room temperature Izod impact strength for ternary blends containing a total of 20 wt% EOR-*g*-MA/EOR mixtures in the rubber phase where the matrix is a-PA (a) and nylon 6 (b).

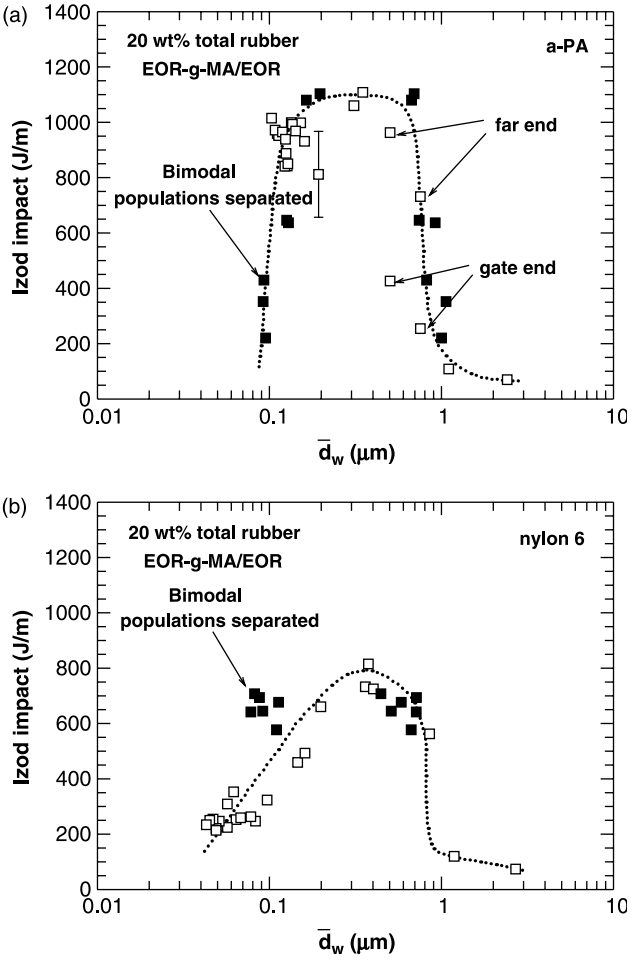

Fig. 3. Effect of weight average rubber particle size on room temperature Izod impact strength for the same ternary blends shown in Fig. 2 except that for blends with a bimodal particle size distribution, particle sizes were evaluated for each of the two populations, and the Izod impact strength is plotted at the size determined for each of the two rubber particle populations for the matrix a-PA (a) and nylon 6 (b).

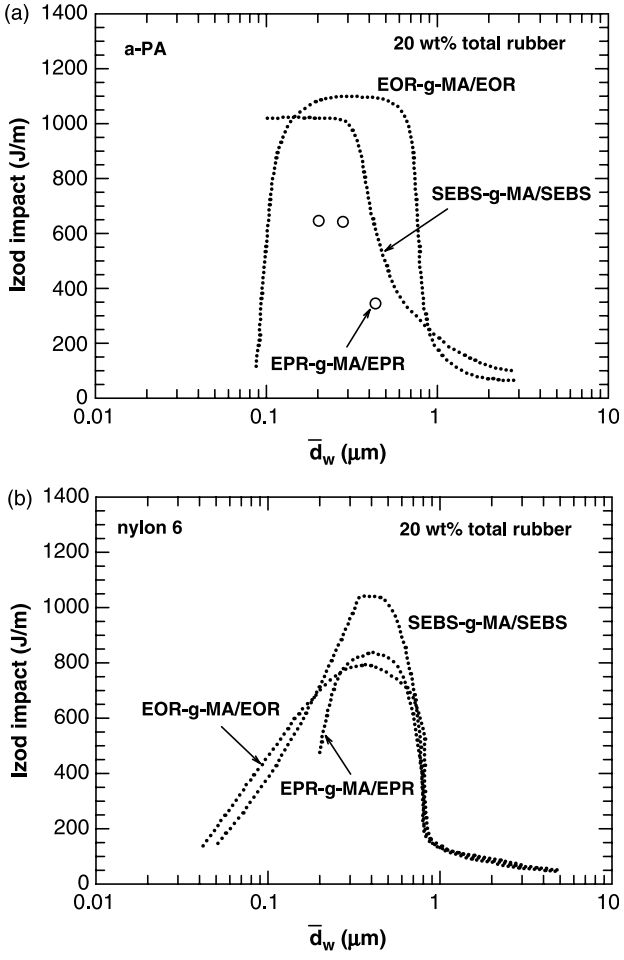

Fig. 4. Comparison of room temperature Izod impact strength as a function of rubber particle size for ternary blends based on three different elastomer systems: EOR-*g*-MA/EOR, EPR-*g*-MA/EPR and SEBS-*g*-MA/SEBS where the total rubber content is fixed at 20 wt% of the blend and a-PA (a) or nylon 6 (b) is the matrix material.

for the population of smaller particles and at the weight average size for the population of large particles. This method of plotting which separates the two populations does not seem to significantly affect the trend observed for nylon 6. However, for a-PA this method of data presentation seems to produce a more coherent relationship showing a well-defined upper and lower particle size limit for toughening.

Instead of using the rubber particle size to correlate the Izod impact strength, Wu proposed the interparticle distance or matrix ligament thickness [3] and provided an equation based on a highly simplified geometric model for calculating the interparticle distance:

$$\tau = d\left[\left(\frac{\pi}{6\phi}\right)^{1/3} - 1\right] \quad (1)$$

where τ is the interparticle distance, d is the rubber particle size and ϕ is the volume fraction of the rubber phase. In the cases discussed above, the volume fraction of the rubber phase is nearly a constant since the total rubber content is fixed at 20 wt% and the maleated and non-maleated EOR elastomers have nearly the same densities. Thus, τ is always proportional to d in this series of blends; thus, the same trend for Izod impact strength versus interparticle distance should exist as the case for Izod impact strength versus rubber particle size. Therefore, plotting versus the interparticle distance adds no new insights in such cases. Furthermore, direct experimental measurement of the average interparticle distance seems much more problematic than determining the average rubber particle size.

Fig. 4 compares the relationships between impact strength versus rubber particle size for three different elastomer systems. For a-PA, all three types of elastomers show an upper limit for toughening beyond which the blend is brittle; the upper size limit seems to be smallest for the EPR-*g*-MA/EPR system and largest for the EOR-*g*-MA/EOR system. Only the EOR-based system shows the lower size limit which is believed to exist for all elastomer systems. It is believed that the lower limit is not observed for EPR and SEBS systems because it was not possible to generate small enough rubber particles in these cases. For nylon 6, however, all three elastomer systems reveal both the upper and lower size limits for toughening. Thus, the optimum range of rubber particle sizes within which the blend is super-tough is well-defined in these cases. This optimum range seems to be nearly the same for EOR-*g*-MA/EOR and SEBS-*g*-MA/SEBS but somewhat narrower for EPR-*g*-MA/EPR. In broad terms, the amorphous polyamide, a-PA, and the semi-crystalline polyamide, nylon 6, show remarkably similar consequences of rubber particle size on toughening behavior. Thus, while crystalline texture certainly may play some role in toughening, it appears that this must be minor since the broad pattern of scale effects seems to be much the same when there is no crystalline structure at all.

4. Effect of temperature on Izod impact strength

Fig. 5 shows Izod impact strength as a function of temperature for binary blends containing varying amounts of EPR-*g*-MA. With addition of EPR-*g*-MA, regardless of the matrix, the blend shows a ductile–brittle transition which shifts to lower temperatures the larger the amount of EPR-*g*-MA added. The ductile–brittle transition temperature responds more strongly to the EPR-*g*-MA content, particularly, at higher contents of rubber for nylon 6 than is the case for a-PA. Fig. 6 shows how impact strength depends on temperature for ternary blends of a-PA where the rubber content is fixed at 20 wt% but the proportions of EPR-*g*-MA and EPR in this phase are varied. The ductile–brittle transition shifts to lower temperatures as the proportion of the maleated component becomes higher. For the blend based on a 20:80 EPR-*g*-MA/EPR mixture, the toughening effect at temperatures above the ductile–brittle transition is quite small.

Fig. 7 shows impact strength versus temperature for ternary blends containing mixtures of EOR-*g*-MA-0.35% with EOR in varying proportions. For a-PA, without EOR-*g*-MA-0.35% in the rubber phase, the blend is brittle at all temperatures examined. The far end specimens are seen to be much tougher than the gate end samples when the two rubbers are in the proportions of 25:75 and 40:60; a clear ductile–brittle

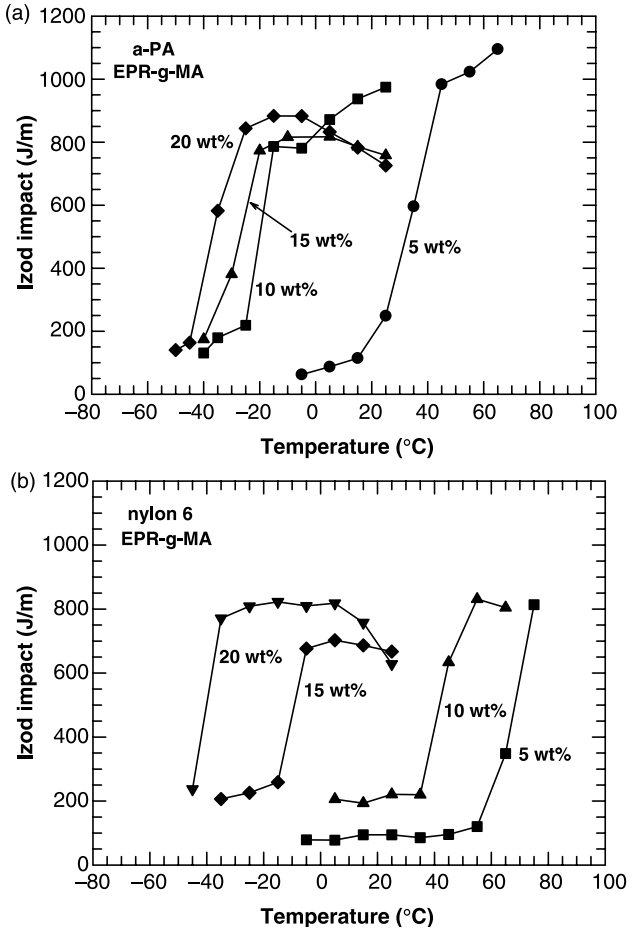

Fig. 5. Izod impact strength as a function of temperature for binary blends with various EPR-*g*-MA contents where the matrix material is a-PA (a) and nylon 6 (b).

transition for these compositions is evident. The transition shifts to a lower temperature with a higher proportion of the maleated component. For nylon 6, a ductile–brittle transition occurs for all the blends and the transition shifts to lower temperatures as the proportion of the maleated component increases. However, the absolute Izod values in the tough regime always seem to be higher for a-PA than for nylon 6.

Fig. 8 shows the Izod impact strength as a function of temperature for ternary blends based on EOR-*g*-MA-2.5%/EOR mixtures as the proportion of the two elastomers is varied. For a-PA, there is a strong ductile–brittle transition which shifts to lower temperatures as the proportion of the maleated component increases. At room temperature, the greater the proportion of maleated elastomer, the tougher the blend. However, the trends for nylon 6 blends are not so simple. The ductile–brittle transition shifts to a lower temperature as the proportion EOR-*g*-MA-2.5%/EOR increases from 16:84 to 60:40. For the blend containing only EOR-*g*-MA-2.5%, there are two transitions, one around 0 °C and the other around 50 °C. The transition around 0 °C is due to the rubber toughening effect but it occurs at a higher temperature than when the rubber phase is diluted with some non-maleated EOR. The change in toughness associated with this transition is

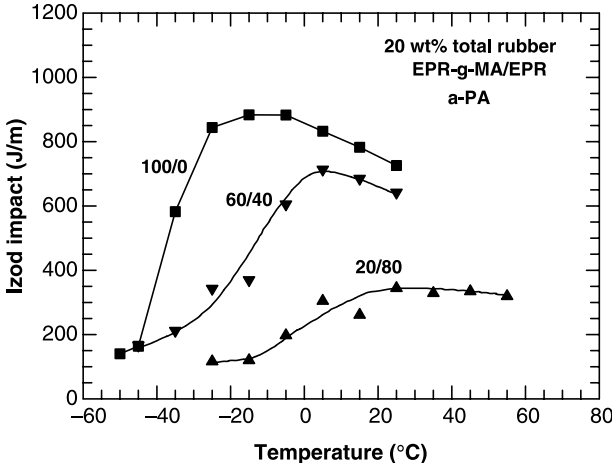

Fig. 6. Izod impact strength versus temperature for ternary blends of a-PA with a total of 20 wt% EPR-*g*-MA/EPR mixture having different proportions in the rubber phase.

rather small. The ductile–brittle transition at higher temperatures is associated with the glass transition of nylon 6 matrix (T_g = 55 °C). As can be seen, the Izod impact strength at room temperature is much lower for nylon 6 than a-PA when the proportion of of EOR-*g*-MA-2.5%/EOR is higher. This can be

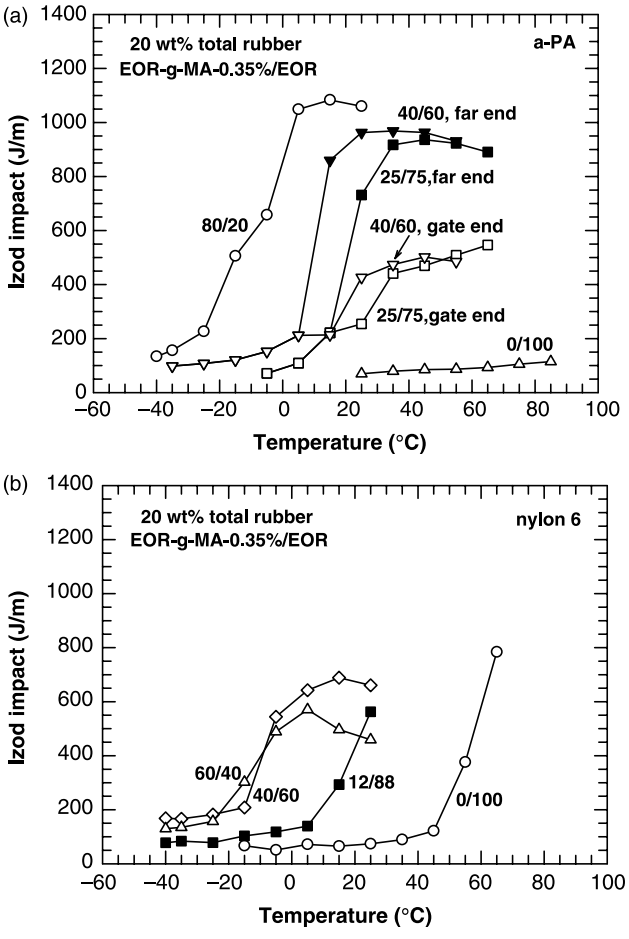

Fig. 7. Effect of temperature on Izod impact strength for ternary blends containing a total of 20 wt% rubber consisting of EOR-*g*-MA-0.35%/EOR mixtures in varying proportions where the matrix is a-PA (a) and nylon 6 (b).

understood in terms of the effect of rubber particle sizes. For a-PA, the rubber particle size of the blends (0.11–0.13 μm) is within the optimum range, whereas for nylon 6 the rubber particle size (0.043–0.062 μm) is below the optimum range for toughening.

Fig. 9 compares the ductile–brittle transition temperature (T_{db}) as a function of EPR-*g*-MA content for binary blends of a-PA and those of nylon 6. In both cases, the T_{db} decreases as the amount of EPR-*g*-MA added increases as expected. Interestingly, the T_{db} is considerably lower for a-PA blends at 5 and 10 wt% EPR-*g*-MA than for nylon 6. However, the difference becomes negligible as the rubber content is about 15 wt% or more. These results suggest that a-PA requires less rubber for effective toughening than does nylon 6.

Many of the trends shown above in terms of rubber phase composition can be unified by analyzing the ductile–brittle transition temperature in terms of average rubber particle size. Fig. 10 shows how T_{db} depends on the rubber particle size for ternary blends based on EOR-*g*-MA/EOR mixtures. For a-PA blends with a unimodal particle size distribution, the ductile–brittle transition temperature decreases greatly with rubber particle size down to about 0.15–0.2 μm, reaches a plateau, and then seems to increase as the particle size become somewhat

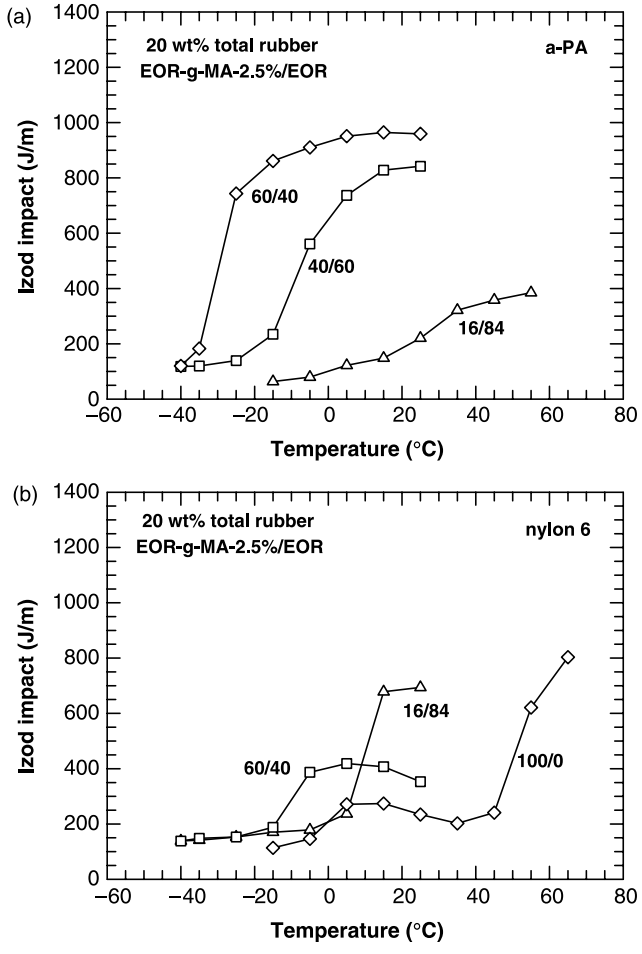

Fig. 8. Izod impact strength versus temperature for ternary blends based on EOR-*g*-MA-2.5%/EOR mixtures in varying proportions when the total rubber phase is fixed at 20 wt% for the matrix a-PA (a) and the matrix nylon 6 (b).

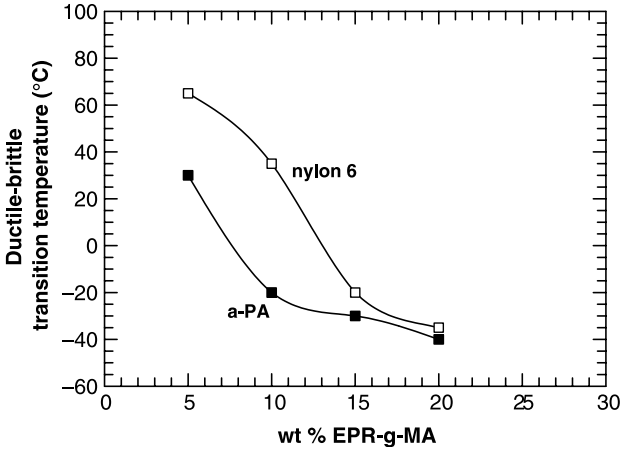

Fig. 9. Effect of the total EPR-*g*-MA content on the ductile–brittle transition temperature for binary blends of EPR-*g*-MA with the matrix material a-PA and nylon 6.

smaller. In this plot, blends that have a bimodal size distribution are represented by a global average size. For a-PA blends with a bimodal particle size distribution, T_{db} is generally higher than that of blends with unimodal distributions. Interestingly, two blends with bimodal distributions have very low ductile–brittle transition temperatures. These two blends are different from other blends showing bimodality in that their degree of bimodality in the two blends is much less developed and the rubber particle size for each population is still within the optimum range for effective toughening. Therefore, the bimodality does not seem to cause any negative effect on toughening, i.e. Izod impact strength and T_{db}. For nylon 6 blends having unimodal size distributions, the ductile–brittle transition temperature decreases gradually with rubber particle size down to about 0.2 μm and then appears to increase gradually at smaller sizes; however, there is a good deal of scatter in the data. The lowest T_{db} observed for nylon 6 with 20 wt% EOR-type rubber is about −20 °C, whereas, a-PA blends show T_{db} as low as −30 °C.

Again, it is useful to re-examine the data in a manner that separates the two populations of rubber particles for blends that show bimodality and plot the single T_{db} at both values of $\bar{d}_w$ for each population. Fig. 11 shows the same data from Fig. 10 plotted in the way similar to the Izod data as shown in Fig. 3. The consequence of plotting the data in this way is to produce what appears to a more well-defined minimum in the plot T_{db} versus $\bar{d}_w$ for both polyamide matrices. Clearly, there is an optimum rubber particle size of the order 0.06–0.20 μm for achieving the lowest possible T_{db}.

Fig. 12 compares the ductile–brittle transition temperatures, as a function of rubber particle size, for blends of the two types of polyamides with three different types of elastomers where the data for a-PA with SEBS-*g*-MA/SEBS are from our previous studies and the data for nylon 6 with EPR-*g*-MA/EPR and SEBS-*g*-MA/SEBS are from Ref. [17]. The dotted lines shown here represent the trends for comparison. For a-PA, the ductile–brittle transition temperature of blends based on EPR-*g*-MA/EPR is about the same as that of blends based on

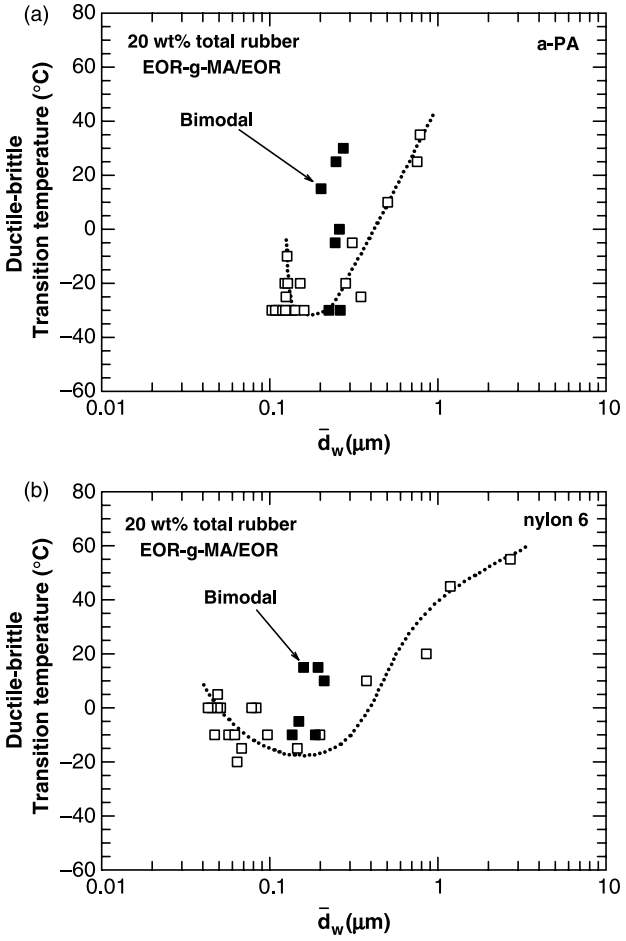

Fig. 10. The ductile–brittle transition temperature as a function of weight average global rubber particle size for ternary blends based on EOR-*g*-MA/EOR mixtures comprised the (20 wt%) rubber phase where the matrix material is a-PA (a) and nylon 6 (b).

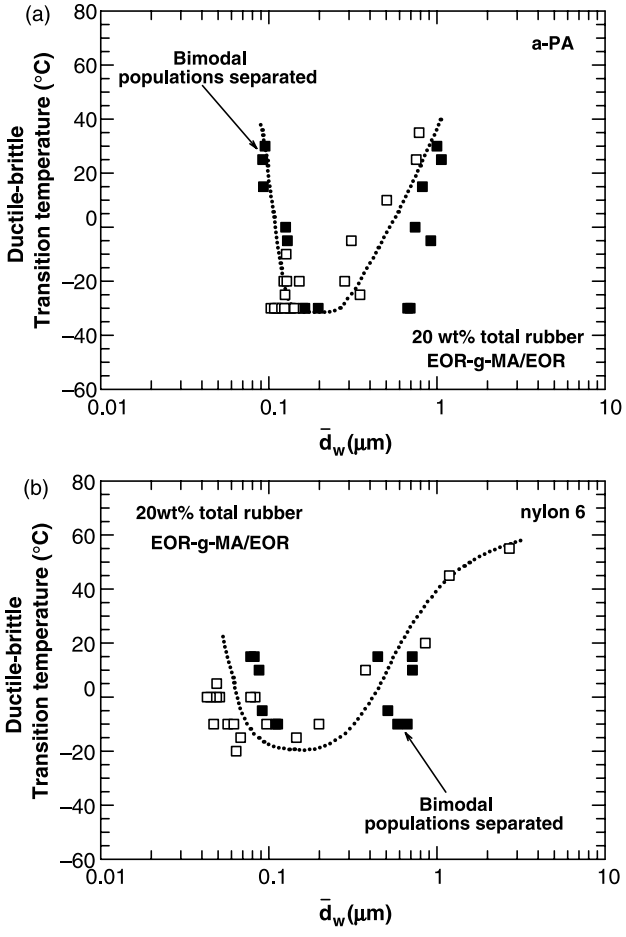

Fig. 11. Effect of weight average rubber particle size on the ductile–brittle transition temperature for the same ternary blend shown in Fig. 10 except that for a blend with a bimodal particle size distribution, a particle size was evaluated for each of the two populations, and the Izod impact strength is plotted at the size computed for each of the two rubber particle populations for the two matrices: a-PA (a) and nylon 6 (b).

EOR-*g*-MA/EOR when compared at the same rubber particle size; however, the limited data for the EPR-*g*-MA/EPR system preclude complete comparison. The T_{db} of blends based on the EOR-*g*-MA/EOR system is lower than that of blends of with SEBS-*g*-MA/SEBS when the rubber particle size is larger than about 0.12 μm. By constrast, the blends with EOR-*g*-MA/EOR have a higher ductile–brittle transition temperature than blends with SEBS-*g*-MA/SEBS, when the particle size is below 0.12 μm. For nylon 6, the EPR-*g*-MA/EPR system always leads to a lower ductile–brittle transition temperature than does EOR-*g*-MA/EOR or SEBS-*g*-MA/SEBS. This difference becomes more significant as the particle size decreases. Lack of data for particle sizes below 0.2 μm for the EPR-*g*-MA/EPR system precludes a more complete comparison. The EOR-*g*-MA/EOR and SEBS-*g*-MA/SEBS systems seem to define a minimum in ductile–brittle transition temperature at a rubber particle size of about 0.15 μm. However, blends with EOR-*g*-MA/EOR have a lower T_{db} than those with SEBS-*g*-MA/SEBS in the region of the optimal particle size. Unfortunately, it was not possible to create small enough rubber particle sizes in the EPR system to see the minimum in T_{db}; however, clearly this elastomer system produces the lowest T_{db} for nylon 6. In the above comparisons, the rubber phase is fixed at 20 wt% in all blend systems. For all blends compared above, the volume fraction is in the range of 24–26% and any variation is believed to be only a negligible factor affecting the comparison.

From the various comparisons shown here, it is clear that in addition to the nature of the matrix and rubber particle size, low temperature toughness is also influenced by the nature of the rubber. Of particular interest here is that the EOR-*g*-MA/EOR system never leads to a ductile–brittle transition temperature in a-PA blends lower than −30 °C or lower than −20 °C in nylon 6 blends, regardless of rubber particle size. On the other hand, the EPR/EPR-*g*-MA system can lead to a ductile–brittle transition temperature of about −40 °C when the matrix is nylon 6. Understanding how the nature of the rubber phase affects the toughness of a blend requires some appreciation of the role of the rubber particles in the toughening mechanisms. The early literature on toughening utilized the idea of stress concentration induced by the presence of low modulus particles dispersed in a more rigid matrix proposed originally for spherical and cylindrical inclusions and later applied to high-impact polystyrene [27,28]. More recently, rubber

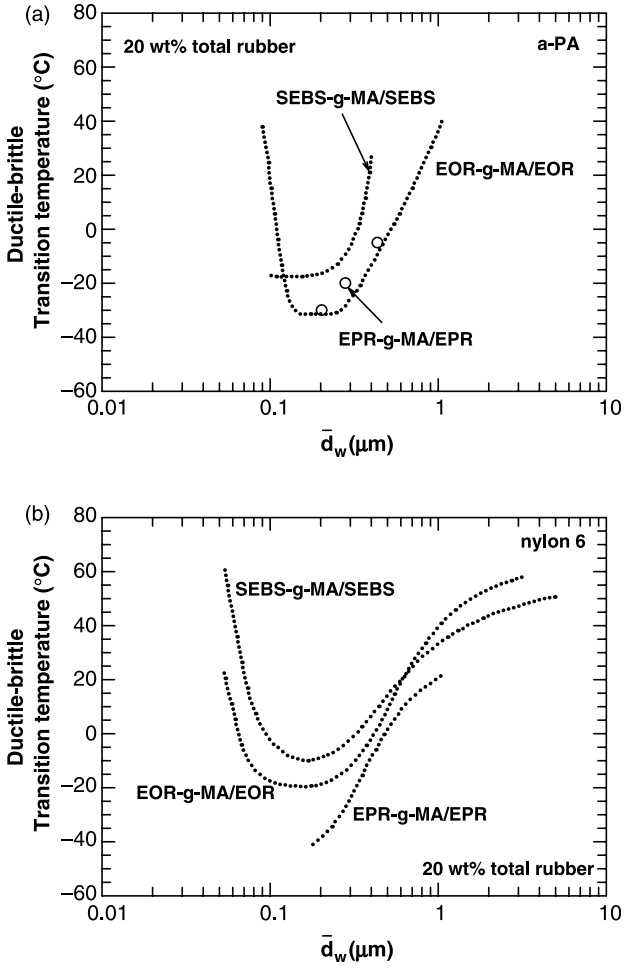

Fig. 12. Comparison of the ductile–brittle transition temperature versus rubber particle size relationship for ternary blends based on three different elastomer systems: EOR-*g*-MA/EOR, EPR-*g*-MA/EPR and SEBS-*g*-MA/SEBS where the total rubber content is fixed at 20 wt% for the matrix material a-PA (a) and nylon 6 (b).

particle cavitation [29–31], which relieves triaxial stress that can trigger shear yielding of pseudo-ductile matrices, has been emphasized. The cavitation of rubber particles no doubt depends on numerous structural parameters, e.g. crosslink density, the microdomain nature of block copolymers, etc. However, to a first approximation, the relative ease of rubber particle cavitation is expected to depend on the modulus of the rubber phase. Clearly, the stiffness of both the matrix and the rubber phase depends on temperature and strongly so in the region of transitions. Thus, examination of the change of modulus in the rubber phase with temperature may be useful in achieving a better understanding of the ductile–brittle transition. An old rule of thumb suggests that the dispersed phase will act as an effective toughener when its modulus is one tenth or less than that of the matrix [1].

The dynamic mechanical property data in Fig. 13 provides a useful basis for examining the ductile–brittle transition temperatures observed here using the simple criterion discussed above. The storage modulus, E', for all the EOR-*g*-MA-*X*% materials are about the same regardless of MA content. However, E' for the EOR-*g*-MA-*X*% materials is much larger than that of EPR-*g*-MA when the temperature is higher than about −57 °C. The maleated EOR elastomers have higher glass transition temperatures than EPR-*g*-MA, as can be seen from the location of the tan δ peaks. The peaks of tan δ for maleated EOR elastomers are quite broader than that of EPR-*g*-MA. The EPR-*g*-MA is an amorphous elastomer as indicated by the manufacturer and by our own observations. The maleated EOR elastomers have a slight amount of crystallinity as revealed by the differential scanning calorimetric (DSC) curves for the four EOR elastomers shown in Fig. 14. There is a broad melting region that peaks at about 75 °C; however, the pre-melting begins well before this. It is difficult to construct a baseline for these DSC scans, but estimates lead to heats of fusion in the range of 58–65 J/g. Using the values of 294 J/g as the heat of fusion for 100% crystalline polyethylene [32] suggests crystallinity levels in the range of 20–22%. Melting of this crystallinity evidently contributes to the breadth of the tan δ peak shown in Fig. 13(b) and the more rapid decline in E' starting at about 20 °C seen in Fig. 13(a).

Fig. 15 shows the ratio of the modulus of a-PA to that of the pure elastomer phase as a function of temperature for each of the maleated elastomers. Based on random ethylene copolymers, as expected, the $E'_{\text{a-PA}}/E'$ ratio decreases as the

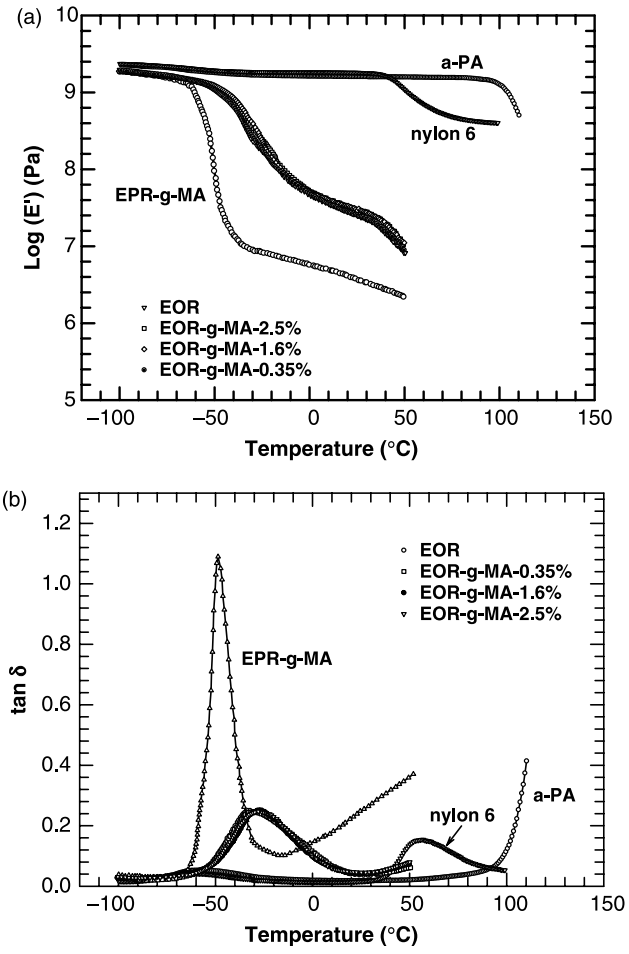

Fig. 13. Dynamic mechanical properties of EOR-*g*-MA-*X*% (*X*=0, 0.35, 1.6, 2.5), EPR-*g*-MA, nylon 6 and a-PA at a frequency of 1 Hz: (a) storage modulus (E') and (b) tan δ.

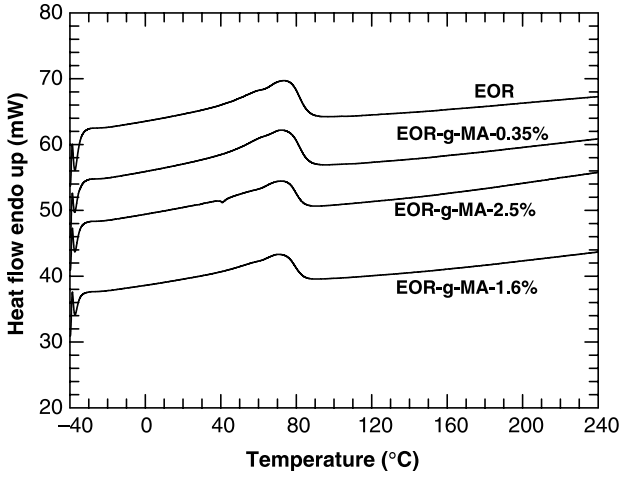

Fig. 14. DSC curves for the four neat EOR elastomers at a scanning rate of 20 °C/min. Data are from the second heating cycle.

temperature is lowered and approaches the order of unity near the T_g of the rubber phase. This ratio is always greater for EPR-*g*-MA than for the EOR-*g*-MA-*X*% materials. If the criterion, $E'_{\text{a-PA}}/E'_{\text{rubber}}=10$, is used, the EPR-*g*-MA material reaches this limit at −50 °C while the EOR-*g*-MA system does so at about −25 °C. These temperatures correspond rather closely to the lowest ductile–brittle temperatures observed for those blends. The glass transition temperature of the rubber phase is often regarded as a lower limit for the ductile–brittle temperature that can be achieved in toughening and that the lower the glass transition temperature in the rubber phase, the lower the ductile–brittle transition temperature of the blend can become. The trend for nylon 6 is similar to that for a-PA with the same rubbers. The maleated EOR materials reach the limit $E'_{\text{nylon6}}/E'_{\text{rubber}}=10$ at about −25 °C while this occurs at −50 °C for EPR-*g*-MA. Again, these values closely correspond to the lowest ductile–brittle transition temperature achieved in these blends. However, the simple criterion, $E'_{\text{matrix}}/E'_{\text{rubber}}=10$ does not unambiguously explain the difference in ductile–brittle temperature observed for a-PA versus nylon 6 blends with the same maleated EOR elastomers, i.e. some blends of a-PA with EOR-*g*-MA/EOR can achieve a ductile–brittle transition temperature of −30 °C, which never occurs for blends of nylon 6 with EOR-*g*-MA/EOR. Clearly, a more detailed consideration is needed to explain such effects, and this is beyond the scope of this study.

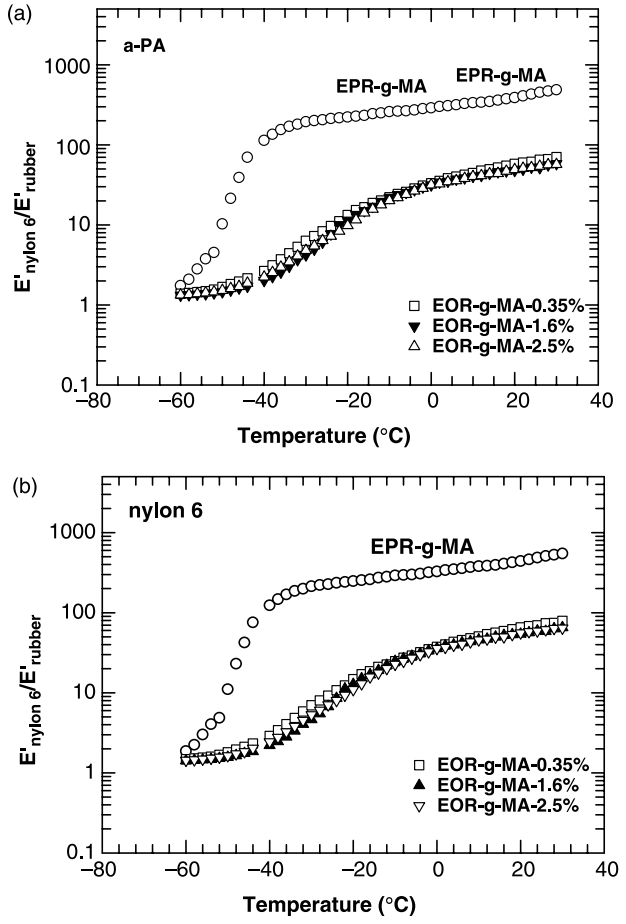

Fig. 15. Ratio of the matrix to rubber moduli, $E'_{\text{matrix}}/E'_{\text{rubber}}$, as a function of temperature for elastomers EOR-*g*-MA-*X*% ($X=0.35$, 1.6, or 2.5) and EPR-*g*-MA for the matrix a-PA (a) or nylon 6 (b).

5. Conclusions

The toughening effect that the two types of elastomers, maleated EPR and EOR, have on two classes of polyamides, semi-crystalline nylon 6 and an amorphous polyamide (Zytel 330), by formation of ternary blends of each of the two polyamides with EPR-*g*-MA/EPR and EOR-*g*-MA/EOR mixtures, has been examined. Izod impact behavior was investigated as a function of rubber content, rubber particle size and temperature. The effect of the three types of elastomer systems including EPR-*g*-MA/EPR, EOR-*g*-MA/EOR, SEBS-*g*-MA/SEBS on impact behavior and the ductile–brittle transition temperature was compared and contrasted for each of the two polyamides. Rubber content significantly influences Izod impact strength; the amorphous polyamide was found to be toughened by a lower content of EPR-*g*-MA than observed for nylon 6. A nearly identical optimum range of rubber particle sizes for effective toughening was observed for both polyamide matrices with the EOR-*g*-MA/EOR system. For a-PA, we were able to fully access the optimum range of rubber particle sizes for toughening at room temperature for the EOR-*g*-MA/EOR elastomer system; however, for the EPR-*g*-MA/EPR and SEBS-*g*-MA/SEBS systems only the upper size limit could be defined since particles small enough to define the lower limit could not be achieved. For a-PA, the upper size limit seems to rank in the order EOR > SEBS > EPR. For nylon 6, all three elastomer systems showed an optimum range of rubber particle sizes, i.e. at room temperature, both upper and lower size limits could be defined. For nylon 6, the optimum size range is nearly the same for EOR-*g*-MA/EOR and SEBS-*g*-MA/SEBS but a more narrow optimum range of particle sizes appears to exist for the EPR-*g*-MA/EPR system. The rubber particle size limits in toughening have been recognized extensively [3,16,33,34]; the lower size limit is usually attributed to the fact that particles are too small to cavitate,

whereas, the upper size limit has been associated with a critical interparticle distance which still remains a controversial topic.

Like Izod impact strength, the ductile–brittle temperature is a strong function of elastomer content and rubber particle size. Higher concentrations of EPR-*g*-MA gave lower ductile–brittle transitions in binary blends with both polyamides. a-PA Binary blends were found to have a much lower ductile–brittle transition temperature than nylon 6 blends when the EPR-*g*-MA content was at or below 10 wt%. This difference seems to diminish at higher contents of rubber. For blends of either of the two polyamide matrices with EOR-*g*-MA/EOR mixtures (at 20 wt% total rubber), the ductile–brittle transition temperature was found to decrease with the particle size to some range and then to increase again.

For blends with a-PA, both the EOR-*g*-MA and EPR-*g*-MA systems led to comparable ductile–brittle transition temperatures within the rubber particle sizes examined. However, the EOR-*g*-MA system showed a minimum in the T_{db} versus particle size relationship. The SEBS-*g*-MA elastomer system also showed a minimum in the T_{db} versus rubber particle size and generally leads to higher ductile–brittle transition temperatures than observed for either of the ethylene-based random copolymer systems. For blends of nylon 6, both EOR-*g*-MA/EOR and SEBS-*g*-MA/SEBS showed a minimum in the T_{db} versus particle size relationship while the ductile–brittle transition temperature for EPR-*g*-MA/EPR system increased monotonically with particle sizes examined. The EPR-*g*-MA/EPR system always showed the lowest T_{db} at the same particle sizes examined.

For blends exhibiting a bimodal particle size distribution, the global weight average rubber particle size was found to be unsuitable for correlating the Izod impact strength and ductile–brittle brittle transition temperature. When plotted versus this global average size, the Izod values tend to be lower than the trend established for blends with a unimodal distribution while the ductile–brittle temperature tends to be higher. Empirically, it was found that plotting the single value of impact strength or T_{db} at the weight average particle size of both the small and large particle populations led to an appealing unification of the data trends. At the present time, we have no fundamental justification for such a graphical representation, but the concept appears to be useful and a better foundation for its use would be interesting to explore.

The lowest possible ductile–brittle transition temperatures achieved for blends with EOR-*g*-MA/EOR mixtures, i.e. at the optimum rubber particle size, seem to be explained rather well in terms of an empirical rule of thumb that to be an effective toughener the rubber phase modulus must be one tenth or less than that of the matrix material. In broad terms, blends with this amorphous polyamide showed rather similar trends (Izod impact or T_{db} versus rubber particle size) to those with semi-crystalline nylon 6, suggesting that any role of crystalline structure of the matrix on toughening must be of secondary importance.

Acknowledgements

The authors are grateful to Dr Jean-Roch Schauder of the European Technology Center, ExxonMobil for valuable technical communications, and to Srivatsan Srinivas of the Baytown Technology and Engineering Complex, ExxonMobil Chemical Company for measuring the density and molecular weight for the four neat EOR elastomers. The authors would thank Honeywell International Inc., E.I. DuPont Co., PolyOne distribution, and ExxonMobil Chemical Co. for donating the materials employed in this work.

References

[1] Epstein BN. US Patent 4, 174, 358 (to E.I. Dupont); 1979.
[2] Borggreve RJM, Gaymans RJ, Schuijer J, Housz JFI. Polymer 1987;28:1489.
[3] Wu S. J Appl Polym Sci 1988;35:549.
[4] Bucknall CB, Heather PS, Lazzeri A. J Mater Sci 1989;24:2255.
[5] Xanthos M. Polym Eng Sci 1988;28:1392.
[6] Pecorini TJ, Manson JA, Hertzberg RW. Polym Prepr 1988;29:136.
[7] Oshinski AJ, Keskkula H, Paul DR. Polymer 1992;33:268.
[8] Oshinski AJ, Keskkula H, Paul DR. Polymer 1992;33:284.
[9] Takeda Y, Keskkula H, Paul DR. Polymer 1992;33:3173.
[10] Dijkstra K, ter Laak J, Gaymans RJ. Polymer 1994;35:315.
[11] Dijkstra K, van der Wal A, Gaymans RJ. J Mater Sci 1994;29:3489.
[12] Majumdar B, Keskkula H, Paul DR. J Appl Polym Sci 1994;54:339.
[13] Majumdar B, Keskkula H, Paul DR. Polymer 1994;35:1386.
[14] Muratoglu OK, Argon AS, Cohen RE, Weinberg M. Polymer 1995;36:921.
[15] Oshinski AJ, Keskkula H, Paul DR. Polymer 1996;37:4891.
[16] Oshinski AJ, Keskkula H, Paul DR. Polymer 1996;37:4909.
[17] Oshinski AJ, Keskkula H, Paul DR. Polymer 1996;37:4919.
[18] Corte L, Beaume F, Leibler L. Polymer 2005;46:2748.
[19] Flexman Jr EA. Polym Eng Sci 1979;19:564.
[20] Borggreve RJM, Gaymans RJ, Eichenwald HM. Polymer 1989;30:78.
[21] Gaymans RJ, van der Werff JW. Polymer 1994;35:3665.
[22] Neuray D, Ott KH. Angew Makromol Chem 1981;98:213.
[23] Epstein BN, Latham RA, Dunphy JF, Pagilagan RU. Elastomerics 1987;119:10.
[24] Huang JJ, Keskkula H, Paul DR. Polymer 2004;45:4203.
[25] Huang JJ, Keskkula H, Paul, DR. Submitted to Polymer.
[26] Huang JJ, Keskkula H, Paul DR. Submitted to Polymer.
[27] Goodier JN. Trans Am Soc Mech Eng 1933;55:39.
[28] Oxborough RJ, Bowden PB. Philos Mag 1974;30:171.
[29] Lazzeri A, Bucknall CB. J Mater Sci 1993;28:6799.
[30] Bucknall CB, Karpodinis A, Zhang XC. J Mater Sci 1994;29:3377.
[31] Dompas D, Groeninckx G. Polymer 1994;35:4743.
[32] Mark HF, Kroschwitz JI.. 2nd ed Encyclopedia of polymer science and engineering, vol. 16. New York: Wiley; 1985.
[33] Bucknall CB. Deformation mechanisms in rubber-toughened polymers. In: Paul DR, Bucknall CB, editors. Polymer blends. 2nd ed. New York: Wiley; 2000. p. 83.
[34] Gaymans RJ. Toughening semicrystalline thermoplastics. In: Paul DR, Bucknall CB, editors. Polymer blends. 2nd ed. New York: Wiley; 2000. p. 177.